Published in final edited form as:
Exp Physiol. 2011 March ; 96(3): 305–316. doi:10.1113/expphysiol.2010.055038.

Activation of the basolateral membrane Cl^- conductance essential for electrogenic K^+ secretion suppresses electrogenic Cl^- secretion

Quanhua He, **Susan T. Halm**, **Jin Zhang**, and **Dan R. Halm**
Department of Neuroscience, Cell Biology & Physiology Wright State University Boonshoft School of Medicine 3640 Colonel Glenn Hwy. Dayton OH 45435

Abstract

Adrenaline activates transient Cl^--secretion and sustained K^+-secretion across isolated distal colonic mucosa of guinea pig. The Ca^{++}-activated Cl^- channel inhibitor CaCCinh-A01 [30μM] significantly reduced electrogenic K^+-secretion, detected as short-circuit current (I_{sc}). This inhibition supported the cell model for K^+-secretion in which basolateral membrane Cl^- channels provide an exit pathway for Cl^- entering the cell via $Na^+/K^+/2Cl^-$-cotransporters. CaCCinh-A01 inhibited both I_{sc} and transepithelial conductance in a concentration dependent manner, IC_{50} = 6.3μM. GlyH-101, another Cl^- channel inhibitor, also reduced sustained adrenaline-activated I_{sc} (IC_{50} = 9.4μM). Adrenaline activated whole-cell Cl^- current in isolated intact colonic crypts, confirmed by ion substitution. This adrenaline-activated whole-cell Cl^- current also was inhibited by CaCCinh-A01 or GlyH-101. In contrast to K^+-secretion, CaCCinh-A01 augmented the electrogenic Cl^--secretion activated by adrenaline as well as that activated by PGE_2. Synergistic Cl^--secretion activated by cholinergic/PGE_2 stimulation was insensitive to CaCCinh-A01. Colonic expression of the Ca^{++}-activated Cl^- channel protein Tmem16A was supported by RT-PCR detection of Tmem16A-mRNA, by immuno-blot with a Tmem16A-antibody, and by immuno-fluorescence detection in lateral membranes of epithelial cells. Alternative splices of Tmem16A were detected for exons that are involved in channel activation. Inhibition of K^+-secretion and augmentation of Cl^--secretion by CaCCinh-A01 supports a common colonic cell model for these two ion secretory processes, such that activation of basolateral membrane Cl^- channels contributes to the production of electrogenic K^+-secretion and limits the rate of Cl^--secretion. Maximal physiological Cl^--secretion occurs only for synergistic activation mechanisms that close these basolateral membrane Cl^- channels.

Keywords

adrenaline; CaCCinh-A01; Tmem16A(Ano1

Introduction

Transepithelial fluid secretion contributes to many physiological processes from digestion to vision (Barrett & Keely, 2006; Planells-Cases & Jentsch, 2009). The composition of the resulting fluid is determined by the very solutes secreted to produce the driving force for water flow. Commonly, electrogenic Cl^--secretion provides the primary cellular event in transepithelial flow such that the fluid is high in NaCl. Activation of Cl^--secretion in each

Corresponding author: Dan R. Halm, NCBP, Wright State University, 3640 Colonel Glenn Hwy, Dayton OH 45435, USA phone: (937) 775-2742 FAX: (937) 775-3391 dan.halm@wright.edu.

organ system occurs via a number of transmitter substances and hormones acting as secretagogs. In the colonic epithelium, many Cl^- secretagogs also activate electrogenic K^+-secretion such that the luminal fluid has a K^+ concentration higher than plasma levels (Halm & Frizzell, 1986; Halm & Rick, 1992; Rechkemmer *etal.*, 1996).

The cellular mechanism producing electrogenic K^+-secretion resembles the standard scheme for Cl^--secretion with the addition of apical membrane K^+ channels (Halm & Frizzell, 1986; Field, 2003). The rate of K^+-secretion depends in part on the relative K^+ conductance of the apical membrane compared with the basolateral membrane. In the limiting case with only apical K^+ channels open (all basolateral K^+ channels closed), the rate of K^+-secretion would approach that of Cl^--secretion. Notably, adrenergic stimulation in the distal colon activates transient Cl^--secretion and sustained K^+-secretion (Zhang *etal.*, 2009b). During the sustained phase of adrenergic activation, K^+-secretion continues in the absence of Cl^--secretion likely because of Cl^- exit across the basolateral membrane. The route of this Cl^- flow appears to occur via Cl^- channels (Halm, 2004). Opening these basolateral Cl^- channels provides an exit path for the Cl^- entering via Na^+-K^+-$2Cl^-$-cotransporters so that a driving force for K^+-secretion is maintained without cell swelling. Just as opening basolateral K^+ channels reduces K^+-secretion, opening these basolateral Cl^- channels could reduce the rate of Cl^--secretion.

The identity of the basolateral membrane Cl^- channels activated during electrogenic K^+-secretion remains unknown. Adrenaline activates single channel currents indicating the presence of several biophysically distinct Cl^- conductance types (Li *etal.*, 2003). Candidates for the channel proteins producing these currents include cAMP-activated Cl^- channels (Cl_{cAMP}) such as CFTR, Ca^{++}-activated Cl^- channels (Cl_{Ca}) such as Tmem16A or bestrophin, as well as the CLC family (Eggermont, 2004; Hartzell *etal.*, 2009; Planells-Cases & Jentsch, 2009; Duran *etal.*, 2010). Small molecule inhibitors of these channels aid in the identification of which types are required for a particular physiological response (Schultz *etal.*, 1999; Verkman & Galietta, 2009). Although many of these inhibitors lack potency and specificity, several have been developed recently using high-through-put-screening including inhibitors for CFTR and Cl_{Ca}. The intent of the present study was to determine the sensitivity of electrogenic K^+-secretion and Cl^--secretion to Cl_{Ca} inhibitors as a means to assess the involvement of Cl^- channels in secretory activation.

Methods

Male guinea pigs (500–800g body weight, Hartley strain; Hilltop Lab Animals, Scottdale PA) received standard chow and water *ad libitum*. Guinea pigs were euthanized with an animal decapitator (Harvard Apparatus, Holliston MA) in accordance with a protocol approved by the Wright State University Laboratory Animal Care and Use Committee. Colonic mucosa was isolated as described previously (Zhang *etal.*, 2009a), and used for measurement of electrical parameters, protein detection by immuno-blot, immunofluorescence, and mRNA expression by RT-PCR.

Transepithelial current measurement

Isolated mucosal sheets were used for measurement of transepithelial current and conductance (Zhang *etal.*, 2009a). Mucosae were mounted in Ussing chambers (0.64cm^2 aperture), supported on the serosal face by nuclepore filters (~10μm thick, 5μm pore diameter; Whatman, Clifton NJ). Bathing solutions (10mL) were circulated by gas-lift through water-jacketed reservoirs (38°C). Standard Ringer's solution contained [in mM]: 145 Na^+, 5.0 K^+, 2.0 Ca^{2+}, 1.2 Mg^{2+}, 125 Cl^-, 25 HCO_3^-, 4.0 $H_{(3-X)}PO_4^{X-}$, 10 D-glucose, continually gassed with 95% O_2 and 5% CO_2 maintaining pH at 7.4. Automatic voltage clamps (Physiologic Instruments, San Diego CA) permitted measurement of short-circuit

current (I_{sc}) and calculation of transepithelial conductance (G_t) from current responses to voltage pulses imposed across the mucosa (±5mV, 3sec duration, 60sec intervals). I_{sc} was referred to as positive for cation flow across the epithelium from mucosal to serosal side.

Responses to secretagogs and inhibitors were obtained from a basal condition produced by suppressing neural and paracrine activators persisting in the isolated mucosa (Zhang *etal.*, 2009b). Briefly, 3 successive replacements of solutions diluted compounds released from the mucosa. The COx-1 (prostaglandin-endoperoxide synthase-1) inhibitor SC-560 [1μM] and COx-2 (PES-2) inhibitor CAY-10404 [1μM] suppressed prostanoid production; the Y2-NpR antagonist BIIE-0246 (1μM, serosal) inhibited PYY/NPY action; amiloride (10μM, mucosal) inhibited electrogenic Na^+ absorption. Sequential addition of secretagogs (adrenaline, prostaglandin-E_2, carbachol) stimulated a range of secretory responses including the *modulatory mode* consisting of electrogenic K^+-secretion alone and *flushing mode* exhibiting high rates of electrogenic Cl^--secretion together with K^+-secretion. Combined stimulation with CCh and PGE_2 produces a super-additive *synergistic mode* of secretion.

Patch-clamp electrical recording

Intact colonic crypts were isolated from mucosal sheets (Li *etal.*, 2003) that were glued to stainless steel holders (0.12mm thick, opening 1cm wide and 4cm long) with cyanoacrylate. These mucosae were incubated in HEPES-buffered solution (38°C), with indomethacin [1μM] to reduce spontaneous fluid and mucus secretion. HEPES-buffered Ringer's solution contained [in mM]: 142 Na^+, 5 K^+, 2 Ca^{++}, 1.2 Mg^{++}, 143 Cl^-, 4 $H_{(3-X)}PO_4^{X-}$, 10 HEPES, 10 D-glucose, continually aerated with 100% O_2. Solutions for separating crypt epithelium from connective tissue contained [in mM]: 192 Na^+, 5 K^+, 97 Cl^-, 4 $H_{(3-X)}PO_4^{X-}$, 10 HEPES, 10 D-glucose and either 30mM citrate or 30mM EDTA. Isolation solution containing EDTA also had 0.1% bovine serum albumin. Mucosae were incubated consecutively in 30mM citrate Ringer (15–30min) and 30mM EDTA Ringer (15–20min). Agitation of holders released crypts into HEPES-buffered Ringer with indomethacin and dithiothreitol [1mM]. Isolated crypts were stored in ice-cold Ringer until use and were suitable for patch-clamp experiments up to ~30h.

Isolated crypts were transferred onto a poly-lysine-coated plastic coverslip in the electrical recording chamber (Warner Instruments, Hamden CT) mounted on the stage of an inverted microscope (Diaphot; Nikon, Melville NY). Pipets with whole-cell solution had resistances of 5–10MΩ. A pipet-holder with a chloridized silver wire (Warner Instruments, Hamden CT) connected to the head-stage of an EPC-9 patch-clamp amplifier (HEKA, Bellmore NY). The reference electrode was a Ag/AgCl pellet connected to the bath through a 150mM-KCl-agar bridge. Seals were made on central tubular portions of crypts bathed in HEPES-buffered Ringer's solution (room temperature), generally 2–10GΩ (Li *etal.*, 2003). Standard whole-cell recording configuration was obtained and currents recorded in response to voltage ramps (200msec) from −100mV to +90mV applied every 2sec holding at −40mV (Liu & Farley, 2007). Standard pipet solution contained [in mM]: 10 Na^+, 150 K^+, 51 Cl^-, 100 $gluconate^-$, 5 HEPES, 0.5 Ca^{++}, 1.0 EGTA. Calculated free Ca^{++} was ~0.4μM. K-free pipet solution contained [in mM]: 8 Na^+, 150 Cs^+, 151 Cl^-, 5 HEPES, 0.5 Ca^{++}, 1.0 EGTA. Cl-free pipet solution contained [in mM]: 10 Na^+, 150 K^+, 151 $gluconate^-$, 5 HEPES, 0.5 Ca^{++}, 1.0 EGTA. Low Cl^- bath solution contained [in mM]: 142 Na^+, 5 K^+, 8 Ca^{++}, 1.2 Mg^{++}, 6 Cl^-, 137 $gluconate^-$, 4 $H_{(3-X)}PO_4^{X-}$, 10 HEPES, 10 D-glucose.

Inhibitors of Cl^- channels were generously provided by R.J. Bridges, Rosalind Franklin University, North Chicago IL (GlyH-101, CFTRinh-172) and A.S. Verkman, University of California, San Francisco CA (CaCCinh-A01). CAY-10404, SC-560, and prostaglandin-E_2 were obtained from Cayman Chemical (Ann Arbor MI); BIIE-0246, CFTRinh-172,

ICI-118551, 5-nitro-2-(3-phenylpropylamino)-benzoate (NPPB) from Tocris Bioscience (Ellisville MO); adrenaline from Hospira (Lake Forest IL). All other chemicals were obtained from Sigma Chemical (St. Louis MO). Drugs were added in small volumes from concentrated stock solutions.

Detection of mRNA and proteins

Total RNA was extracted by RNeasy-Mini-Kit (Qiagen, Valencia CA) from isolated mucosa and EDTA-released epithelial cells prepared as for patch-clamp recording. Briefly (Zhang *etal*., 2009a), after reverse transcription of mRNA, cDNA was amplified by PCR: initial denaturing 95°C (10min), 40 cycles denaturation 92°C (1 min), annealing 64°C (1 min), extension 72°C (8min). Primers specific for Cl_{Ca}-Tmem16A were based on previous design (Ferrera *etal.*, 2009; O'Driscoll *etal.*, 2010) and alignment of nucleotide sequences for human, mouse, and rat (GenBank accession NM_018043, NM_178642, NM_001107564). Primers for the exon6B-segment were *forward* 5'-cag-aag-atc-aca-gac-ccc-atc-c-3' and *reverse* 5'-cag-gga-tga-gca-tct-ggg-tgt-3', exon15-segment *forward* 5'-acg-aag-cca-gag-tct-tgg-ag-3' and *reverse* 5'-caa-act-tca-gca-gga-aag-cc-3', and exon6/exon16-segment *forward* 5'-gaa-caa-cgt-gca-cca-agg-cca-agt-a-3' and *reverse* 5'-tgg-tga-aat-agg-ctg-gga-atc-ggt-c-3'.

Proteins were isolated from colonic epithelial cells. Briefly (Zhang *etal.*, 2009a), after disruption by sonication in a buffered solution containing protease inhibitors, samples were centrifuged to obtain a membrane sample. Following SDS-PAGE and transfer to polyvinylidene difluoride membranes, incubation with Cl_{Ca}-Tmem16A specific primary antibody (1:500, rabbit monoclonal SP31 of human *Ano1*; ab64085, Abcam Inc, Cambridge MA), and then with horseradish peroxidase-conjugated secondary antibody (Jackson ImmunoResearch Laboratories, West Grove PA) allowed detection of protein.

Immuno-fluorescence localization in colonic mucosa followed previous methods (Zhang *etal*., 2009a). Briefly, isolated mucosal sheets were immersed in fixation solutions, dehydrated, sectioned, mounted on gelatin-coated slides, permeabilized/blocked, and then incubated for 24 h (4°C) with primary antibody for Cl_{Ca}-Tmem16A (6.7ng/μL, rabbit polyclonal of human *Ano1*; ab53212, Abcam Inc, Cambridge MA). A donkey-anti-rabbit IgG antibody, conjugated to AlexaFluor®488 (Invitrogen, Carlsbad CA), was used to detect immuno-reactivity (4ng/μL, 2hr, room temp). Sections were washed, mounted in Vectashield (Vector Labs, Burlingame CA), and fluorescence visualized with an Olympus BX60 epifluorescence microscope.

Data Analysis

Responses of I_{sc} and G_t to secretagogs and antagonists were obtained from adjacent mucosae in each colon to permit direct comparisons. I_{sc} recordings were digitized at 10sec intervals to examine secretory time courses. Concentration dependences were fit by Henri-Michaelis-Menten binding curves using non-linear least-squares procedures. Patch-clamp data were analyzed using FitMaster software (HEKA, Bellmore NY). Band intensities were analyzed using ImageJ software. Results were reported as mean and standard error of the mean (sem) with the number of animals (n) indicated. Statistical comparisons were made using a two-tailed Student's t-test for paired responses (experimental – control), with significant difference accepted at $P<0.05$.

Results

Action of Cl^- channel inhibitors on β-adrenergic activated ion secretion

Adrenaline (adr) stimulates a transient positive I_{sc} component ($^{adr}I_{sc}$) associated with Cl^--secretion and a sustained negative $^{adr}I_{sc}$ associated with K^+-secretion (Zhang *etal.*, 2009b).

The Ca^{++}-activated Cl^- channel (Cl_{Ca}) inhibitor CaCCinh-A01 used at a concentration ~3-fold higher than the reported IC_{50} (De La Fuente *etal.*, 2008) rapidly decreased the basal negative I_{sc} toward zero consistent with inhibiting K^+-secretion (Fig 1A). Subsequent adrenaline activation in the presence of CaCCinh-A01 produced transient positive $^{adr}I_{sc}$ without sustained negative $^{adr}I_{sc}$. These results conformed to the cell model for K^+-secretion requiring basolateral membrane Cl^- channels (Halm, 2004), but contradicted the concept that Cl_{Ca} in the apical membrane supports Cl^--secretion (Eggermont, 2004; Hartzell *etal.*, 2009). The presence of the cAMP-activated Cl^- channel CFTR (Cl_{cAMP}-CFTR) in the apical membrane also often contributes to Cl^--secretion (Barrett & Keely, 2006; Duran *etal.*, 2010), such that Cl_{cAMP}-CFTR and Cl_{Ca} together would determine the secretory rate. The peak of the adrenaline activated Cl^- secretory transient was indistinguishable in the presence or absence of the Cl_{cAMP}-CFTR inhibitor CFTRinh-172 [30μM] ($\Delta^{adr}I_{sc}$= +13.8±14.8μA/cm^2, n=4, P=0.42). This result with CFTRinh-172 at a concentration ~30-fold higher than the IC_{50} (Verkman & Galietta, 2009) indicated an insensitivity of the apical membrane Cl^- channels supporting Cl^--secretion, either due to a specific insensitivity of guinea pig colonic CFTR or the lack of CFTR involvement in this response. Including both CaCCinh-A01 and CFTRinh-172 also produced a secretory transient indistinguishable from control activation (data not shown). The sustained negative $^{adr}I_{sc}$ associated with K^+-secretion was indistinguishable in the presence or absence of CFTRinh-172 [30μM] ($\Delta^{adr}I_{sc}$=+7.1±3.4μA/cm^2, n=4, P=0.13), further supporting the selective action of CaCCinh-A01.

β-adrenergic activation of Cl^--secretion requires β2-adrenergic receptors (β2-AdrR), such that the selective β2-AdrR antagonist ICI-118551 eliminates positive transient $^{adr}I_{sc}$ leaving unaltered the sustained $^{adr}I_{sc}$ associated with K^+-secretion (Halm *etal.*, 2010). In the presence of ICI-118551, CaCCinh-A01 addition inhibited sustained K^+ secretory $^{adr}I_{sc}$ (Fig 1B). The concentration dependence provided an IC_{50} of 6.3μM for CaCCinh-A01 inhibition of $^{adr}I_{sc}$ (Fig 1C); G_t also decreased in a concentration dependent manner (data not shown). The Cl_{cAMP}-CFTR/Cl_{Ca} inhibitor GlyH-101 (Verkman & Galietta, 2009) acted with similar efficacy. NPPB also inhibits some Cl_{Ca} (Eggermont, 2004) and reduced $^{adr}I_{sc}$; but at concentrations >10μM, large increases in G_t occurred suggesting an additional action compromising epithelial integrity. Niflumate, another inhibitor of Cl_{Ca}, reduced $^{adr}I_{sc}$ (IC_{50} ~50μM) with the caveat that concentrations ≥30μM compromised G_t as with NPPB (data not shown, n=3). The channel blocker DPC (diphenylamine-2-carboxylate; Schultz *etal.*, 1999) inhibited less strongly (IC_{50} ~150μM, data not shown, n=3). The lack of inhibition by CFTRinh-172 on negative $^{adr}I_{sc}$ supported an IC_{50} of >500μM. This pattern of inhibitor sensitivity observed for K^+ secretory $^{adr}I_{sc}$ conformed to that reported for Cl_{Ca} (Eggermont, 2004; Hartzell *etal.*, 2009), supporting an involvement of Cl_{Ca} as part of the basolateral Cl^- conductance required for electrogenic K^+-secretion.

Adrenaline activated whole-cell currents

Basal currents from cells of intact crypts had linear current-voltage relations, recorded using a standard whole-cell configuration (Fig 2A). Adrenaline addition to the bathing solution increased currents with a shift of the reversal potential to more negative values consistent with stimulation of K^+ conductance. Adrenaline stimulation of Cl^- currents (I_{Cl}) was apparent at E_K, since K^+ currents would be zero. Using a CsCl pipet solution to eliminate K^+ current, whole-cell recordings produced currents reversing near zero in basal and adrenaline stimulated conditions consistent with Cl^- currents (Fig 2B). Addition of CaCCinh-A01 to the bath reduced I_{Cl} to basal levels. This CaCCinh-A01 sensitive current had a nearly linear current-voltage relation. Activation of I_{Cl} by adrenaline was rapid after a variable delay of 10–90sec, which likely resulted from mixing in the chamber (Fig 2C), and $^{adr}I_{Cl}$ remained stable for over 10min. The ionic identity of $^{adr}I_{Cl}$ was supported by its continued presence during K^+ replacement by Cs^+ and its absence during Cl^- replacement by gluconate$^-$. The

Cl^- channel inhibitors CaCCinh-A01, GlyH-101, and NPPB rapidly decreased this inward current during adrenaline activation (Fig 2D) consistent with blockade of $^{adr}I_{Cl}$.

Action of Cl^- channel inhibitors on Cl^--secretion

Insensitivity of β-adrenergic activated Cl^--secretion to the Cl^- channel blocker CaCCinh-A01 (Fig 1A) supported a secretory model involving distinct Cl^- channel types in apical and basolateral membranes. Inhibiting basolateral membrane Cl^- channels in a Cl^- secretory cell would have immediate consequences. Since the component of $^{adr}I_{sc}$ sensitive to β2-AdrR antagonism is Cl^--secretion (Halm *etal.*, 2010), comparing ICI-118551-sensitive $^{adr}I_{sc}$ for experimental and control mucosae indicated that CaCCinh-A01 augmented Cl^--secretion at all time points (Fig 3A). This result supported a secretory model in which basolateral membrane Cl^- channels contribute to the control of Cl^- secretory rate by redirecting a portion of intracellular Cl^- back into the interstitial space. CaCCinh-A01 also augmented PGE_2 stimulation of Cl^--secretion (Fig 3B) indicating that basolateral membrane Cl^- channels were active during stimulation with other Cl^--secretagogs. Synergistic activation of Cl^--secretion with combined PGE_2 and cholinergic stimulation was augmented by CaCCinh-A01 only at the 1st peak of I_{sc} but not at the 2ndpeak or during the plateau (Fig 3C). Thus, the mechanism of synergistic activation likely included inhibition of basolateral membrane Cl^- channels, which would maximize conductive exit of Cl^- across the apical membrane.

Other Cl^- channel inhibitors tested also exhibited some ability to augment Cl^--secretion. GlyH-101 [10μM] significantly enhanced the 1st and 2nd peaks of the positive $^{adr}I_{sc}$ similar to CaCCinh-A01 (Table 1). During subsequent PGE_2 stimulation GlyH-101 increased the 1st and 2nd peaks leaving the plateau unaltered. In contrast, GlyH-101 inhibited synergistic stimulation (CCh/PGE_2) at the 1st peak, 2nd peak, and plateau consistent with inhibition of apical membrane Cl^- channels during the synergistic secretory mode. Adding NPPB (at 10μM to exclude toxic effects) left unaltered the adrenaline 1st and 2nd peaks as well as the 1st peaks of PGE_2 and synergistic activation. NPPB [10μM] enhanced the 2nd peak and plateau of PGE_2 activation while inhibiting the synergistic 2nd peak and plateau. Lower efficacy for niflumate (IC_{50}>30μM) combined with increased G_t at ≥30μM made evaluation of action on Cl^--secretion ambiguous, but it was qualitatively similar to GlyH-101 (data not shown). Neither CFTRinh-172 (30μM, n=4) nor DPC (100μM, n=3) altered the positive I_{sc} responses to adrenaline, PGE_2 or synergistic activation (data not shown).

Expression of the Ca^{++}-activated Cl^- channel Tmem16A

Presence of Cl_{Ca}-Tmem16A in colonic epithelial cells was detected by immuno-blot (Fig 4A). Two bands were apparent, consistent with a fully dissociated monomer and a larger oligomer possibly containing two monomers or a monomer and tightly adherent accessory protein (Galietta, 2009). Brain expresses Cl_{Ca}-Tmem16A (Ferrera *etal.*, 2009) and guinea pig brain lysate exhibited a band at the smaller size seen in colon (Fig 4A), similar to that in portal vein smooth muscle (Davis *etal.*, 2010).

RT-PCR of mRNA from colonic mucosa (Fig 4B) confirmed the presence of Cl_{Ca}-Tmem16A (Flores *etal.*, 2009;Yu *etal.*, 2010) and demonstrated splicing events. Guinea pig exon-6B had an amino-acid sequence identical to human Cl_{Ca}-Tmem16A (Fig 4C); three amino-acids with positively charged side chains (RKK) differ in mouse and rat exon-6B by a substitution of the central lysine with arginine (RRK). Of the 8 possible splicing combinations for the mRNA segment between exon-6 and exon-16 (Ferrera *etal.*, 2009;O'Driscoll *etal.*, 2010), the dominant transcript in colonic epithelial cells included exon-6B and exon-13 without exon-15 (Figs 4D &4E; GenBank accession HQ341643). The minor apparent transcript including exon-15 (Fig 4B) was not detected among the products

of this longer segment (Fig 4D). The smaller transcript present in mucosal samples (Fig 4D) likely omitted both exon-6B and exon-15 and occurred in a non-epithelial cell population.

The cellular location of Cl_{Ca}-Tmem16A was determined by immuno-fluorescence microscopy. In both surface and crypt cells, Cl_{Ca}-Tmem16A immuno-reactivity (ir) was observed as puncta that were consistent with a presence in lateral membranes (Fig 5). Similar clustering of labeling is seen with Cl_{Ca}-Tmem16A expressed in HEK293 cells (Kunzelmann *etal.*, 2009). Evidence of Cl_{Ca}-Tmem16A^{ir} was not apparent along the luminal margins of the surface and crypt cells, suggesting an absence of Cl_{Ca}-Tmem16A from the apical membrane.

Discussion

Epithelia involved in fluid secretion generally produce electrogenic Cl^--secretion using apical membrane Cl^- channels as the route for Cl^- exit from the cell into the lumen of a duct or gland (Field, 2003; Barrett & Keely, 2006). Any basolateral membrane Cl^- channels would likely be considered as contributing to cell volume regulation during swelling events. In the case of colonic electrogenic K^+-secretion, basolateral Cl^- channels are an integral part of the secretory mechanism by providing a route for exit after uptake via Na^+-K^+-$2Cl^-$-cotransporters and by contributing to setting the electro-chemical driving forces for K^+ and Cl^- exit (Li *etal.*, 2003; Halm, 2004; Fig 6). The Ca^{++}-activated Cl^- channel (Cl_{Ca}) inhibitor CaCCinh-A01 (De La Fuente *etal.*, 2008) inhibited K^+-secretion consistent with an action on basolateral Cl^- channels (Fig 1B). Specificity of CaCCinh-A01 for these basolateral channels over apical Cl^- channels was apparent by the lack of overt inhibitory action on electrogenic Cl^--secretion (Fig 1A).

A pharmacological definition of the basolateral Cl^- channels involved in K^+-secretion provides a means to compare with specific channel types (Planells-Cases & Jentsch, 2009; Verkman & Galietta, 2009; Duran *etal.*, 2010). The non-steroidal anti-inflammatory drugs DPC and niflumate inhibit Cl^- channels with low potency, but led to the first generation Cl^- channel inhibitor NPPB (Wangemann *etal.*, 1986). Recent high-throughput strategies produced higher potency inhibitors for CFTR and Cl_{Ca} (De La Fuente *etal.*, 2008; Verkman & Galietta, 2009). Although CFTRinh-172 and GlyH-101 were optimized for CFTR inhibition, GlyH-101 also inhibits Cl_{Ca}-Tmem16A (Caputo *etal.*, 2008). The order of inhibitor efficacy for K^+-secretion (Fig 1C; CaCCinh-A01 > GlyH-101 > NPPB ≈ niflumate > DPC ≫ CFTRinh-172) matched best with the sensitivity of Cl_{Ca} (Eggermont, 2004; Hartzell *etal.*, 2009).

The Cl_{Ca}-Tmem16A protein behaves similar to the Cl_{Ca} described in many cell types of native tissues (Eggermont, 2004; Galietta, 2009; Hartzell *etal.*, 2009). Splice variants alter the Ca^{++}-sensitivity and current-voltage characteristics (Caputo *etal.*, 2008; Ferrera *etal.*, 2009) such that different combinations of Cl_{Ca}-Tmem16A proteins may account for the observed range of Cl_{Ca} behavior. In particular, both outwardly rectified and linear Cl_{Ca} have been observed. Present in many tissues, Cl_{Ca}-Tmem16A occurs in colonic epithelial cells together with other members of the Tmem16 family (Flores *etal.*, 2009; Yu *etal.*, 2010). The dominant form of Cl_{Ca}-Tmem16A in guinea pig distal colonic epithelial cells included exons 6B and 13 but lacked exon-15 (Fig 4D). Although absence of exon-15 from Cl_{Ca}-Tmem16A does not alter expressed channel function, the presence of exon-13 confers outward rectification (Ferrera *etal.*, 2009). The linear current-voltage dependence of crypt cell $^{adr}I_{Cl}$ (Fig 2) is inconsistent with this feature of Cl_{Ca}-Tmem16A. However, other modifications may alter conductance properties. The 146kDa guinea pig Cl_{Ca}-Tmem16A protein (Fig 4A) was similar to the expressed size (Schreiber *etal.*, 2010) and may represent the monomer with tightly associated accessory proteins (Galietta, 2009). With the lower

Ca^{++} sensitivity conferred by exon-6B (Ferrera *etal.*, 2009), β-adrenergic elevation of cytosolic Ca^{++} (del Castillo *etal.*, 1999) could account for the activation of CaCCinh-A01-sensitive $^{adr}I_{Cl}$ in crypt cells (Figs 2 & 4C).

The inhibitor sensitivity profile of Cl_{Ca} and Cl_{Ca}-Tmem16A provides a direct means to assess channel involvement in K^+-secretion. Niflumate inhibition is commonly used to indicate a possible requirement for Cl_{Ca}, and K^+-secretion shares a similar sensitivity to niflumate (Figs 1C) with Cl_{Ca}-Tmem16A and Cl_{Ca} (Caputo *etal.*, 2008;Schröder *etal.*, 2008). Both Tmem16A (Caputo *etal.*, 2008) and K^+-secretion share sensitivity to GlyH-101 which further supports a mechanistic connection. Also, the lack of CFTRinh-172 inhibition for Cl_{Ca}-Tmem16A and K^+-secretion suggested an absence of CFTR involvement in K^+-secretion. Although the potent inhibition of K^+-secretion by CaCCinh-A01 supported a requirement for Cl_{Ca}, limited testing of Cl_{Ca}-Tmem16A with this inhibitor makes the comparison tentative (Almaça etal., 2009). Overall, the inhibitor sensitivity of K^+-secretion (Fig 1C) and $^{adr}I_{Cl}$ (Fig 2) supported Cl_{Ca}-Tmem16A as the most likely channel responsible for the adrenaline-activated basolateral membrane Cl^- conductance (Fig 6).

Basolateral membrane Cl^- currents have been recorded in colonic epithelial cells possibly involved in NaCl absorption and volume regulation (Schultheiβ & Diener, 1998; Mignen *etal.*, 2000). Sensitivity to NPPB suggested a general similarity with $^{adr}I_{Cl}$ (Fig 2). CLC-2 likely contributes to the basolateral Cl^- conductance supporting NaCl absorption and predominantly appears in surface cells (Peña-Münzenmayer *etal.*, 2005). Patients with cystic fibrosis exhibit electrogenic K^+-secretion in response to Cl^- secretagogs (Goldstein *etal.*, 1991; Mall *etal.*, 2000) supporting the presence of basolateral Cl^- channels in secretory cells of the colon. Double knockout mice for CFTR and CLC-2 produce a lower apparent rate of K^+-secretion compared with CFTR knockout mice suggesting that CLC-2 contributes to basolateral Cl^- conductance involved in K^+-secretion (Zdebik *etal.*, 2004). Another manifestation of K^+-secretion appears in patients with acute colonic pseudo-obstruction (Jetmore *etal.*, 1992; Camilleri & Szarka, 2009). The K^+ wasting observed (van Dinter *etal.*, 2005; Blondon *etal.*, 2008) likely results from prolonged sympathetic activation of K^+-secretion. Distinctions between these Cl^- channels in the basolateral membranes and those found in the apical membrane (Fig 6) likely would allow for independent cellular regulation mechanisms and provide the possibility for specific pharmaceutical intervention.

In contrast with electrogenic K^+-secretion which requires activation of basolateral membrane Cl^- channels, electrogenic Cl^--secretion requires activation of apical membrane Cl^- channels (Fig 6). Together, CFTR and Cl_{Ca} often account for this apical Cl^- conductance (Eggermont, 2004;Duran *etal.*, 2010), although some secretagogs likely activate other apical Cl^- channels (Hoque *etal.*, 2010). The demonstration of Cl_{Ca}-Tmem16A in the apical membrane of salivary gland cells (Romanenko *etal.*, 2010;Yang *etal.*, 2008) and airway epithelium (Huang *etal.*, 2009) together with Tmem16A-null mice exhibiting suppressed cholinergic-activated Cl^--secretion (Ousingsawat *etal.*, 2009) supports Cl_{Ca}-Tmem16A as an apical Cl^- channel. In addition, the Cl_{Ca} inhibitor CaCCinh-A01 inhibits purinergic-activated Cl^--secretion in colonic T84-cells (De La Fuente *etal.*, 2008;Tradtrantip *etal.*, 2010) and airway epithelial cells (Namkung *etal.*, 2010). Perhaps an example of species differences, Cl_{Ca}-Tmem16A was not apparent in the apical membrane of guinea pig colon epithelium (Fig 5) and Cl^--secretion was insensitive to CaCCinh-A01 inhibition (Table 1) supporting a lack of apical involvement by this Cl_{Ca}.Cl^--secretion also was insensitive to CFTRinh-172, although CFTR is present in guinea pig colon (Stewart *etal.*, 2009) and Cl^- currents in guinea pig pancreatic ducts are sensitive to CFTRinh-172 (Park *etal.*, 2010). The apparent absence of CFTR and Cl_{Ca}-Tmem16A contributions imply that other Cl^- channel types support the observed electrogenic Cl^--secretion. The inhibitor profile for synergistic mode Cl^--secretion (CCh/PGE_2, Table 1) supports the presence of

apical Cl^- channels sensitive to GlyH-101 and NPPB but insensitive to CaCCinh-A01, possibly a Cl_{Ca} other than Cl_{Ca}-Tmem16A.

Dramatically, CaCCinh-A01 augmented both adrenergic and prostanoid activated Cl^--secretion (Fig 3) supporting a common cellular model for Cl^--secretion and K^+-secretion in which basolateral Cl^- channels provide an important route for Cl^- exit (Fig 6). A similar concept has been proposed for airway epithelial cells with the suggestion that CLC-2 and bestrophin play major roles in the basolateral membrane Cl^- conductance (Duta *etal.*, 2006;Fischer *etal.*, 2007). For the colonic epithelium, the actions of CaCCinh-A01 supported a Cl_{Ca} as the dominant basolateral Cl^- channel involved in secretory regulation. The lack of CaCCinh-A01 augmentation for the synergistic mode of Cl^--secretion (Fig 3C) supports an activation mechanism in which maximal Cl^--secretion occurs by inhibiting this basolateral Cl^- conductance such that all Cl^- exit occurs across the apical membrane (Fig 6C). Indeed, the standard conceptualization of Cl^- secretion most closely matches the synergistic mode with its maximization of apical Cl^- exit. Intermediate rates of Cl^--secretion would be produced not only by graded opening of apical Cl^- channels but also by coordinated opening of basolateral Cl^- channels (Fig 6A).

β-adrenergic activation of ion secretion in the distal colon illustrates the switching between Cl^--secretion and K^+-secretion that occurs using basolateral Cl^- channels (Fig 1). Early activation includes opening of apical and basolateral Cl^- channels so that the rate of Cl^--secretion is modest compared with other secretagogs (Fig 6A). The transient nature of β-adrenergic Cl^--secretion occurs as apical Cl^- channels close until reaching the sustained phase when only basolateral Cl^- channels remain open, which still allows K^+-secretion to continue (Fig 6B). Although both Cl^--secretion and K^+-secretion require cAMP for activation, the adenylyl cyclases producing the cAMP are distinct for the two types of secretion indicating a divergence of signaling for apical and basolateral Cl^- channels (Halm *etal.*, 2010). Since neuropeptide receptor signaling also suppresses Cl^--secretion (Zhang *etal.*, 2009b), the colonic epithelium can adjust the rates of Cl^--secretion and K^+-secretion by several mechanisms.

Acknowledgments

This study was supported by a grant from the National Institutes of Health, National Institute of Diabetes and Digestive and Kidney Diseases (DK65845). The authors thank M. Di Fulvio for helpful discussions on expression studies.

References

Almaça J, Tian Y, Aldehni F, Ousingsawat J, Kongsuphol P, Rock JR, Harfe BD, Schreiber R, Kunzelmann K. TMEM16 proteins produce volume-regulated chloride currents that are reduced in mice lacking TMEM16A. J Biol Chem. 2009; 284:28571–28578. [PubMed: 19654323]

Barrett, KE.; Keely, SJ. Integrative physiology and pathophysiology of intestinal electrolyte transport. In: Johnson, LR., editor. Physiology of the Gastrointestinal Tract. Raven Press; New York: 2006. p. 1931-1951.

Blondon H, Béchade D, Desramé J, Algayres JP. Secretory diarrhoea with high faecal potassium concentrations: a new mechanism of diarrhoea associated with colonic pseudo-obstruction? Report of five patients. Gastroenterol Clin Biol. 2008; 32:401–404. [PubMed: 18394839]

Camilleri, M.; Szarka, L. Dysmotility of the small intestine and colon. In: Yamada, T., editor. Textbook of Gastroenterology. 5th ed. Blackwell Pub; Hoboken, NJ: 2009. p. 1108-1156.

Caputo A, Caci E, Ferrera L, Pedemonte N, Barsanti C, Sondo E, Pfeffer U, Ravazzolo R, Zegarra-Moran O, Galietta LJ. TMEM16A, a membrane protein associated with calcium-dependent chloride channel activity. Science. 2008; 322:590–594. [PubMed: 18772398]

Davis AJ, Forrest AS, Jepps TA, Valencik ML, Wiwchar M, Singer CA, Sones WR, Greenwood IA, Leblanc N. Expression profile and protein translation of TMEM16A in murine smooth muscle. Am J Physiol Cell Physiol. 2010; 299:C948–C959. [PubMed: 20686072]

De La Fuente R, Namkung W, Mills A, Verkman AS. Small-molecule screen identifies inhibitors of a human intestinal calcium-activated chloride channel. Mol Pharmacol. 2008; 73:758–68. [PubMed: 18083779]

del Castillo JR, Arévalo JC, Burguillos L, Súlbaran-Carrasco MC. β-adrenergic agonists stimulate Na^+-K^+-Cl^- cotransport by inducing intracellular Ca^{++} liberation in crypt cells. Am J Physiol Gastrointest Liver Physiol. 1999; 277:G563–G571.

Duran C, Thompson CH, Xiao Q, Hartzell HC. Chloride channels: often enigmatic, rarely predictable. Annu Rev Physiol. 2010; 72:95–121. [PubMed: 19827947]

Duta V, Duta F, Puttagunta L, Befus AD, Duszyk M. Regulation of basolateral Cl^- channels in airway epithelial cells: the role of nitric oxide. J Membr Biol. 2006; 213:165–174. [PubMed: 17468957]

Eggermont J. Calcium-activated chloride channels: (un)known, (un)loved? Proc Am Thorac Soc. 2004; 1:22–27. [PubMed: 16113407]

Ferrera L, Caputo A, Ubby I, Bussani E, Zegarra-Moran O, Ravazzolo R, Pagani F, Galietta LJ. Regulation of TMEM16A chloride channel properties by alternative splicing. J Biol Chem. 2009; 284:33360–33368. [PubMed: 19819874]

Field M. Intestinal ion transport and the pathophysiology of diarrhea. J Clin Invest. 2003; 111:931–943. [PubMed: 12671039]

Fischer H, Illek B, Finkbeiner WE, Widdicombe JH. Basolateral Cl channels in primary airway epithelial cultures. Am J Physiol Lung Cell Mol Physiol. 2007; 292:L1432–L1443. [PubMed: 17322286]

Flores CA, Cid LP, Sepúlveda FV, Niemeyer MI. TMEM16 proteins: the long awaited calcium-activated chloride channels? Braz J Med Biol Res. 2009; 42:993–1001. [PubMed: 19784506]

Galietta LJ. The TMEM16 protein family: a new class of chloride channels? Biophys J. 2009; 97:3047–3053. [PubMed: 20006941]

Goldstein JL, Shapiro AB, Rao MC, Layden TJ. In vivo evidence of altered chloride but not potassium secretion in cystic fibrosis rectal mucosa. Gastroenterology. 1991; 101:1012–1019. [PubMed: 1679733]

Halm DR. Secretory control of basolateral membrane potassium and chloride channels in colonic crypt cells. Adv Exp Med Biol. 2004; 559:119–129. [PubMed: 18727233]

Halm DR, Frizzell RA. Active K^+ transport across rabbit distal colon: relation to Na^+ absorption and Cl^- secretion. Am J Physiol Cell Physiol. 1986; 251:C252–C267.

Halm DR, Rick R. Secretion of K^+ and Cl^- across colonic epithelium: cellular localization using electron microprobe analysis. Am J Physiol Cell Physiol. 1992; 262:C1001–C1011.

Halm ST, Zhang J, Halm DR. β-adrenergic activation of electrogenic K^+ and Cl^- secretion in guinea pig distal colonic epithelium proceeds via separate cAMP signaling pathways. Am J Physiol Gastrointest Liver Physiol. 2010; 299:G81–G95. [PubMed: 20413718]

Hartzell HC, Yu K, Xiao Q, Chien LT, Qu Z. Anoctamin/TMEM16 family members are Ca^{++}-activated Cl^- channels. J Physiol. 2009; 587:2127–2139. [PubMed: 19015192]

Hoque KM, Woodward OM, van Rossum DB, Zachos NC, Chen L, Leung GPH, Guggino WB, Guggino SE, Tse C-M. Epac1 mediates protein kinase A-independent mechanism of forskolin-activated intestinal chloride secretion. J Gen Physiol. 2010; 135:43–158. [PubMed: 20038525]

Huang F, Rock JR, Harfe BD, Cheng T, Huang X, Jan YN, Jan LY. Studies on expression and function of the TMEM16A calcium-activated chloride channel. Proc Natl Acad Sci USA. 2009; 106:21413–21418. [PubMed: 19965375]

Jetmore AB, Timmcke AE, Gathright JB Jr, Hicks TC, Ray JE, Baker JW. Ogilvie's syndrome: colonoscopic decompression and analysis of predisposing factors. Dis Colon Rectum. 1992; 35:1135–1142. [PubMed: 1473414]

Kunzelmann K, Kongsuphol P, Aldehni F, Tian Y, Ousingsawat J, Warth R, Schreiber R. Bestrophin and TMEM16-Ca^{++} activated Cl^- channels with different functions. Cell Calcium. 2009; 46:233–241. [PubMed: 19783045]

Li Y, Halm ST, Halm DR. Secretory activation of basolateral membrane Cl^- channels in guinea pig distal colonic crypts. Am J Physiol Cell Physiol. 2003; 284:C918–C933. [PubMed: 12505791]

Liu H, Farley JM Sr. Prostaglandin E_2 enhances acetylcholine-induced, Ca^{++}-dependent ionic currents in swine tracheal mucous gland cells. J Pharmacol Exp Ther. 2007; 322:501–513. [PubMed: 17483294]

Mall M, Wissner A, Seydewitz HH, Kühr J, Brandis M, Greger R, Kunzelmann K. Defective cholinergic Cl^- secretion and detection of K^+ secretion in rectal biopsies from cystic fibrosis patients. Am J Physiol Gastrointest Liver Physiol. 2000; 278:G617–G624. [PubMed: 10762616]

Mignen O, Egee S, Liberge M, Harvey BJ. Basolateral outward rectifier chloride channel in isolated crypts of mouse colon. Am J Physiol Gastrointest Liver Physiol. 2000; 279:G277–G287. [PubMed: 10915635]

Namkung W, Finkbeiner WE, Verkman AS. CFTR-adenylyl cyclase I association responsible for UTP activation of CFTR in well-differentiated primary human bronchial cell cultures. Mol Biol Cell. 2010; 21:2639–2648. [PubMed: 20554763]

O'Driscoll KE, Hatton WJ, Britton FC. Alternative splicing of the murine Tmem16a transcript in heart. FASEB J. 2010; 24:1002.28.

Ousingsawat J, Martins JR, Schreiber R, Rock JR, Harfe BD, Kunzelmann K. Loss of TMEM16A causes a defect in epithelial Ca^{++}-dependent chloride transport. J Biol Chem. 2009; 284:28698–28703. [PubMed: 19679661]

Park HW, Nam JH, Kim JY, Namkung W, Yoon JS, Lee JS, Kim KS, Venglovecz V, Gray MA, Kim KH, Lee MG. Dynamic regulation of CFTR bicarbonate permeability by $[Cl^-]_i$ and its role in pancreatic bicarbonate secretion. Gastroenterology. 2010; 139:620–631. [PubMed: 20398666]

Peña-Münzenmayer G, Catalán M, Cornejo I, Figueroa CD, Melvin JE, Niemeyer MI, Cid LP, Sepúlveda FV. Basolateral localization of native ClC-2 chloride channels in absorptive intestinal epithelial cells and basolateral sorting encoded by a CBS-2 domain di-leucine motif. J Cell Sci. 2005; 118:4243–4252. [PubMed: 16155254]

Planells-Cases R, Jentsch TJ. Chloride channelopathies. Biochim Biophys Acta. 2009; 1792:173–189. [PubMed: 19708126]

Rechkemmer G, Frizzell RA, Halm DR. Active K^+ transport across guinea pig distal colon: action of secretagogues. J Physiol. 1996; 493:485–502. [PubMed: 8782111]

Romanenko VG, Catalán MA, Brown DA, Putzier I, Hartzell HC, Marmorstein AD, Gonzalez-Begne M, Rock JR, Harfe BD, Melvin JE. Tmem16A encodes the Ca^{++}-activated Cl^- channel in mouse submandibular salivary gland acinar cells. J Biol Chem. 2010; 285:12990–3001. [PubMed: 20177062]

Schreiber R, Uliyakina I, Kongsuphol P, Warth R, Mirza M, Martins JR, Kunzelmann K. Expression and function of epithelial anoctamins. J Biol Chem. 2010; 85:7838–7845. [PubMed: 20056604]

Schröder BC, Cheng T, Jan YN, Jan LY. Expression cloning of TMEM16A as a calcium-activated chloride channel subunit. Cell. 2008; 134:1019–1029. [PubMed: 18805094]

Schultheiβ G, Diener M. K^+ and Cl^- conductances in the distal colon of the rat. Gen Pharmacol. 1998; 31:337–342. [PubMed: 9703198]

Schultz BD, Singh AK, Devor DC, Bridges RJ. Pharmacology of CFTR chloride channel activity. Physiol Rev. 1999; 79:S109–S144. [PubMed: 9922378]

Stewart AK, Yamamoto A, Nakakuki M, Kondo T, Alper SL, Ishiguro H. Functional coupling of apical Cl^-/HCO_3^- exchange with CFTR in stimulated HCO_3^- secretion by guinea pig interlobular pancreatic duct. Am J Physiol Gastrointest Liver Physiol. 2009; 296:G1307–G1317. [PubMed: 19342507]

Tradtrantip L, Namkung W, Verkman AS. Crofelemer, an antisecretory antidiarrheal proanthocyanidin oligomer extracted from Croton lechleri, targets two distinct intestinal chloride channels. Mol Pharmacol. 2010; 77:69–78. [PubMed: 19808995]

van Dinter TG Jr, Fuerst FC, Richardson CT, Ana CA, Polter DE, Fordtran JS, Binder HJ. Stimulated active potassium secretion in a patient with colonic pseudo-obstruction: a new mechanism of secretory diarrhea. Gastroenterology. 2005; 129:1268–1273. [PubMed: 16230079]

Verkman AS, Galietta LJ. Chloride channels as drug targets. Nat Rev DrugDiscov. 2009; 8:153–171.

Wangemann P, Wittner M, Di Stefano A, Englert HC, Lang HJ, Schlatter E, Greger R. Cl^--channel blockers in the thick ascending limb of the loop of Henle: Structure activity relationship. Pflugers Arch. 1986; 407(Suppl 2):S128–141. [PubMed: 2434915]

Yang YD, Cho H, Koo JY, Tak MH, Cho Y, Shim WS, Park SP, Lee J, Lee B, Kim BM, Raouf R, Shin YK, Oh U. TMEM16A confers receptor-activated calcium-dependent chloride conductance. Nature. 2008; 455:1210–1215. [PubMed: 18724360]

Yu K, Lujan R, Marmorstein A, Gabriel S, Hartzell HC. Bestrophin-2 mediates bicarbonate transport by goblet cells in mouse colon. J Clin Invest. 2010; 120:1722–1735. [PubMed: 20407206]

Zdebik AA, Cuffe JE, Bertog M, Korbmacher C, Jentsch TJ. Additional disruption of the ClC-2 Cl^- channel does not exacerbate the cystic fibrosis phenotype of cystic fibrosis transmembrane conductance regulator mouse models. J Biol Chem. 2004; 279:22276–22283. [PubMed: 15007059]

Zhang J, Halm ST, Halm DR. Adrenergic activation of electrogenic K^+ secretion in guinea pig distal colonic epithelium: involvement of β1- and β2-adrenergic receptors. Am J Physiol Gastrointest Liver Physiol. 2009a; 297:G269–G277. [PubMed: 19460844]

Zhang J, Halm ST, Halm DR. Adrenergic activation of electrogenic K^+ secretion in guinea pig distal colonic epithelium: desensitization via the Y2-neuropeptide receptor. Am J Physiol Gastrointest Liver Physiol. 2009b; 297:G278–G291. [PubMed: 19497958]

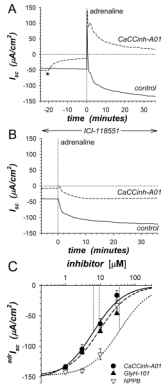

Figure 1. Inhibition of K^+-secretion by CaCCinh-A01

A. I_{sc} (see Methods) was measured in adjacent isolated mucosae without (solid line) or with (dashed line) CaCCinh-A01 [30μM] added to mucosal and serosal baths ~20min prior to adrenaline [5μM] stimulation (*). I_{sc} was significantly different between control and CaCCinh-A01 treated for basal conditions prior to adrenaline addition (ΔI_{sc}= +36.6±3.1μA/cm^2, n=4, P<0.002), as well as at the 1st peak, 2nd peak, and steady-state plateau (Table 1). **B.** The action of CaCCinh-A01 [30μM] on I_{sc} during adrenaline stimulation ($^{adr}I_{sc}$) was measured as in panel A with ICI-118551 [0.3μM] present to suppress transient positive I_{sc}. **C.** Inhibitory responses of CaCCinh-A01 (●, n=4), GlyH-101 (▲, n=4), and NPPB (▽, n=3) for $^{adr}I_{sc}$ were measured in adjacent mucosae with ICI-118551 [0.3μM], by cumulative increases from 1μM to 30μM during steady-state activation. Fits of Henri-Michaelis-Menton kinetics (single binding site) were made to the resulting concentration dependences of $^{adr}I_{sc}$: $^{CaCCinh}EC_{50}$=6.3±1.4μM, $^{GlyH}EC_{50}$=9.4±0.7μM, $^{NPPB}EC_{50}$=36±9μM, with each significantly different from the others (P<0.05).

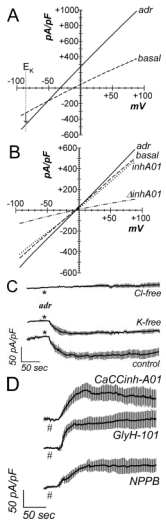

Figure 2. Adrenaline activated Cl^- currents

A. Isolated colonic crypts were stimulated by adrenaline [10μM] during standard whole-cell patch-clamp recording (see Methods): adrenaline (solid line), basal level (dashed line). Increased Cl^- current was apparent at the K^+ reversal potential (E_K). **B.** Adrenaline stimulated current with pipet solution K^+ replaced with Cs^+, consistent with activated Cl^- current. Addition of CaCCinh-A01 [50μM] reduced current to basal levels. **C.** Adrenaline stimulated (*) inward current measured at E_K (−86mV) with an activation $\tau_{0.5}$ of ~14sec (I_{Cl}, mean±sem, n=17). Variable delay in onset was adjusted by aligning the times at which I_{Cl} began increasing. Similar activation occurred in the absence of K^+ (CsCl pipet, n=8). Substitution of Cl^- in the recording solutions eliminated the response (n=4); currents were aligned at the time of adrenaline addition. **D.** Cl^- channel blockers (#) inhibited the adrenaline-activated inward current (added 3–5min earlier). The $\tau_{0.5}$ of inhibition was ~20sec for CaCCinh-A01 (50μM, n=3), ~18sec for GlyH-101 (50μM, n=3), and ~30 sec for NPPB (100μM, n=3).

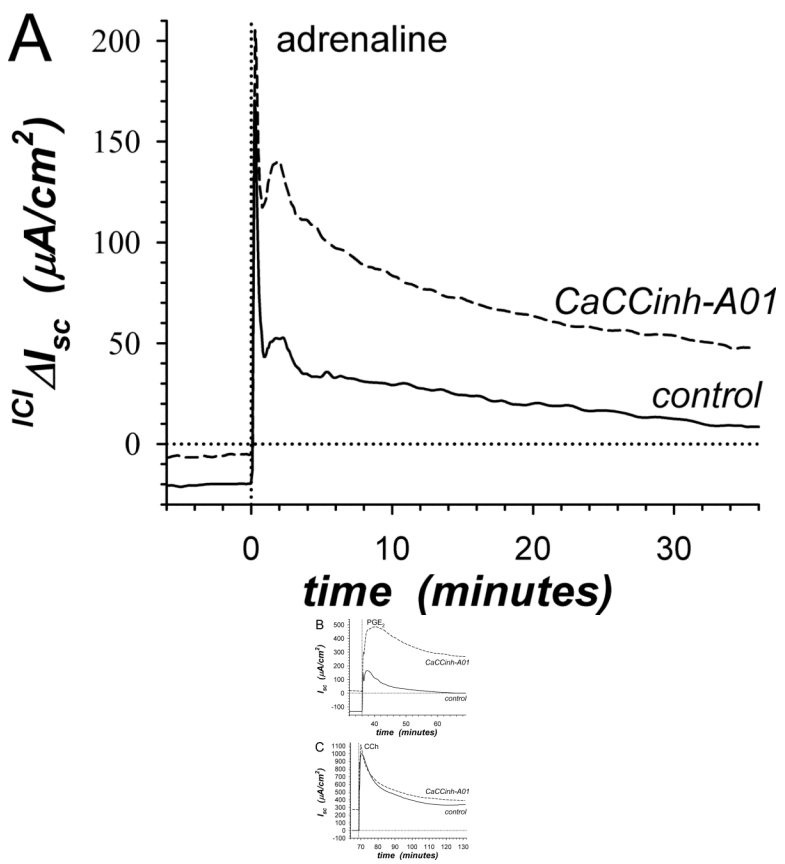

Figure 3. Stimulation of Cl^--secretion by CaCCinh-A01

A. The action of CaCCinh-A01 [30μM] on the positive $^{adr}I_{sc}$ component was obtained from 4 adjacent mucosae stimulated as in Fig 1. The difference of $^{adr}I_{sc}$ ($^{ICI}\Delta I_{sc}$) with and without ICI-118551 [0.3μM] provided the β2-AdrR Cl^- secretory response: control (solid line), CaCCinh-A01 (dashed line). **B.** Adjacent mucosae were stimulated with adrenaline [5μM] (0min) followed by PGE_2 [3μM] without (solid line) or with CaCCinh-A01 (dashed line). **C.** Adjacent mucosae were stimulated with adrenaline (0min) and PGE_2 (36min) followed by CCh [10μM] without (solid line) or with CaCCinh-A01 (dashed line).

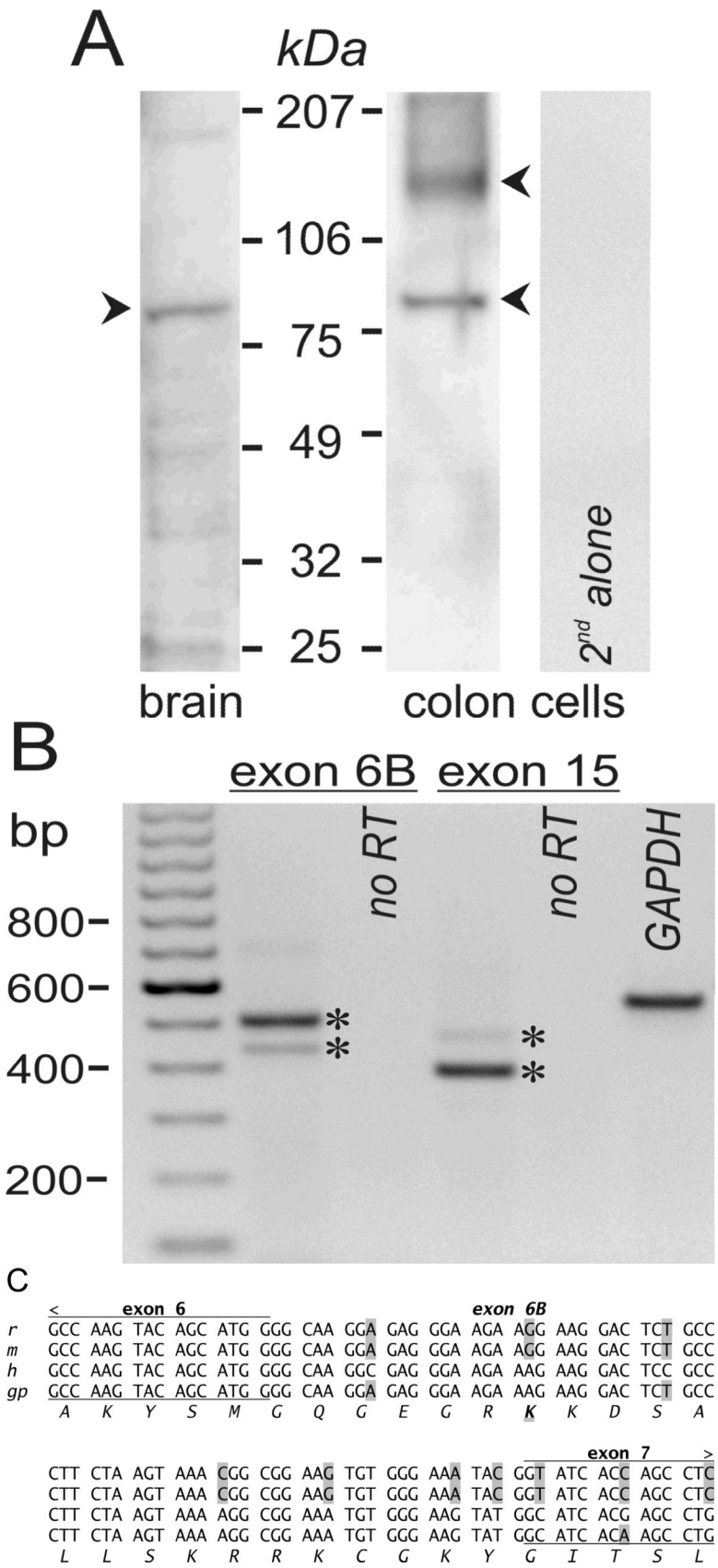

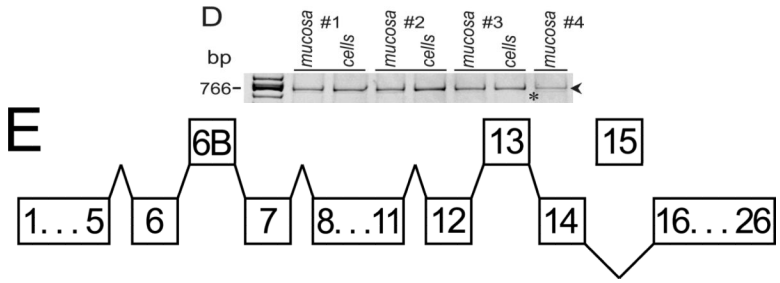

Figure 4. Expression of Ca^{++}-activated Cl^{-} channel Tmem16A

A. Immuno-blots of the membrane fraction from distal colonic epithelial cells with anti-Tmem16A(*Ano1*) exhibited bands at 85kDa and 146kDa (arrowheads). These bands were not apparent with the secondary antibody alone, indicating that the primary antibody was necessary to observe results. A cell lysate of guinea pig brain exhibited a band at 84kDa. **B.** RT-PCR of mucosal mRNA amplified Tmem16A(*Ano1*) products with sizes predicted by the position of the primers (asterisks), 504 base pairs for the segment including exon-6B and 395-base-pairs for the segment omitting exon-15. The faint exon-6B product likely represented a splice variant lacking exon-6B, 438bp; and, the faint exon-15 product likely represented a splice variant including exon-15, 473bp. Sequencing of products confirmed identity with Tmem16A (homology: 87% human, 88% mouse, 87% rat). Amplification of GAPDH product (555bp) served as positive control for RNA isolation. Absence of product when not including reverse transcriptase indicated the lack of genomic DNA contamination. **C.** The sequence of the insert designated as variant-b (Ferrera *etal.*, 2009) is labeled exon-6B and shown for rat, mouse, human, and guinea pig, with differences from human indicated by shading. **D.** In mucosa and epithelial cell samples from 4 colons, the dominant Tmem16A product from exon-6 to exon-16 (~770bp, arrowhead) was consistent with a transcript including exon-6B and exon-13 while omitting exon-15 (confirmed by sequencing; GenBank accession HQ341643). A smaller faint band (~710bp, asterisk) was consistent with a transcript including exon-13 and omitting both exon-6B and exon-15, and was 11±2% (n=4) of the total product in mucosa and 1±1% (n=3) of the total in epithelial cells. Markers were 900, 800, 766, and 600 base pairs. **E.** The exons of Tmem16A are shown schematically (alternatively spliced exons above), with the transcript in guinea pig distal colonic epithelial cells including exon-6B and exon-13 while omitting exon-15. The sequenced portion spans exon-4 to exon-16.

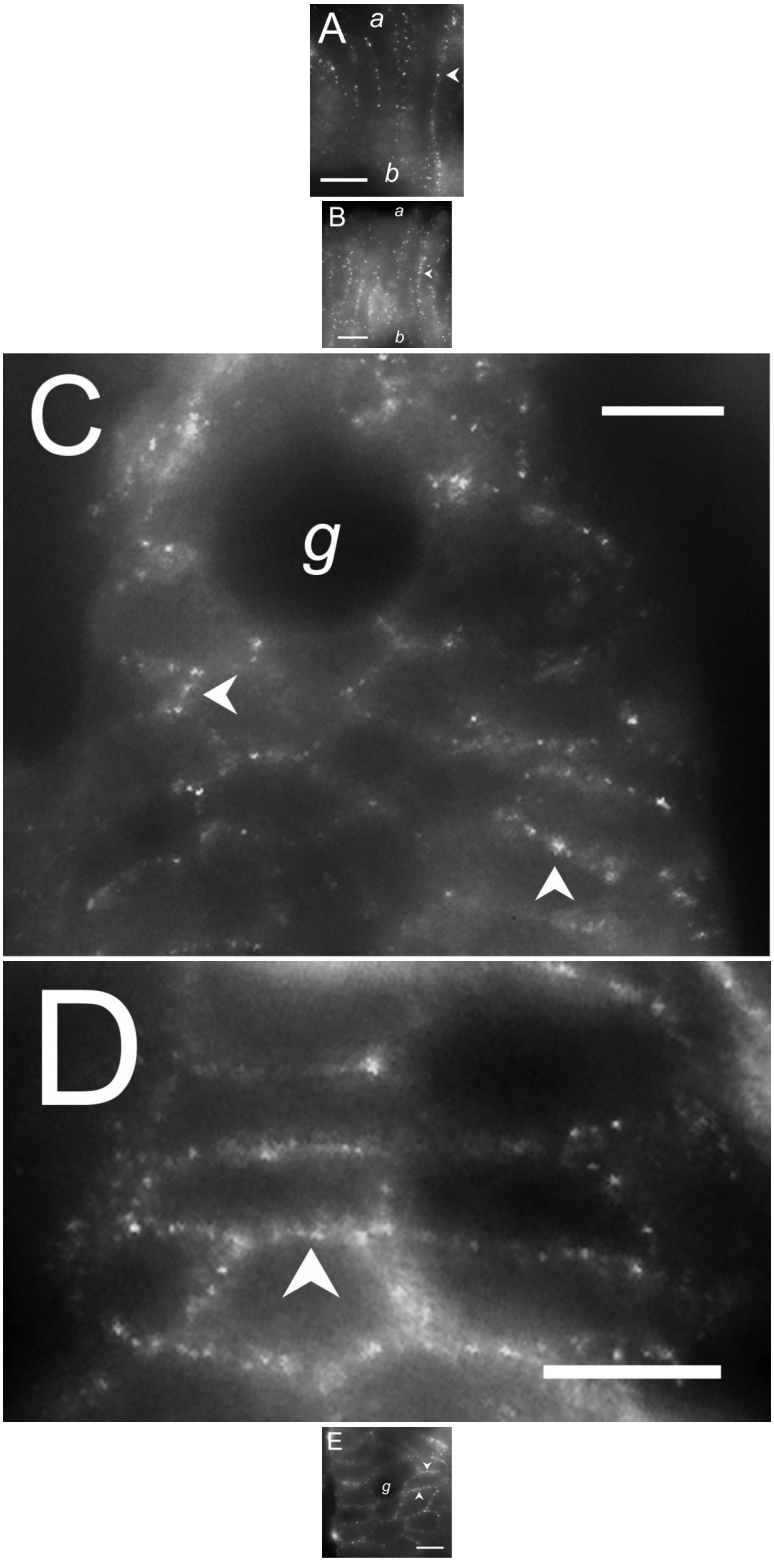

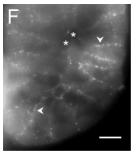

Figure 5. Localization of the Tmem16A Ca^{++}-activated Cl^{-} channel

Tmem16A protein was detected by immuno-fluorescence in distal colon mucosa. **A.** & **B.** Surface epithelial cells had prominent $Tmem16A^{ir}$ labeling of lateral membranes (arrowheads). Labeling of apical (*a*) or basal (*b*) membranes was not apparent. **C.** – **F.** Crypts showed distinct lateral membrane $Tmem16A^{ir}$ labeling (arrowheads). Luminal margins lacked labeling (asterisk). Apically located goblet granule masses were apparent as dark voids (*g*). Use of the secondary antibody alone eliminated all labeling (data not shown), indicating that the primary antibody was necessary for the observed results. Scale bars, 10μm.

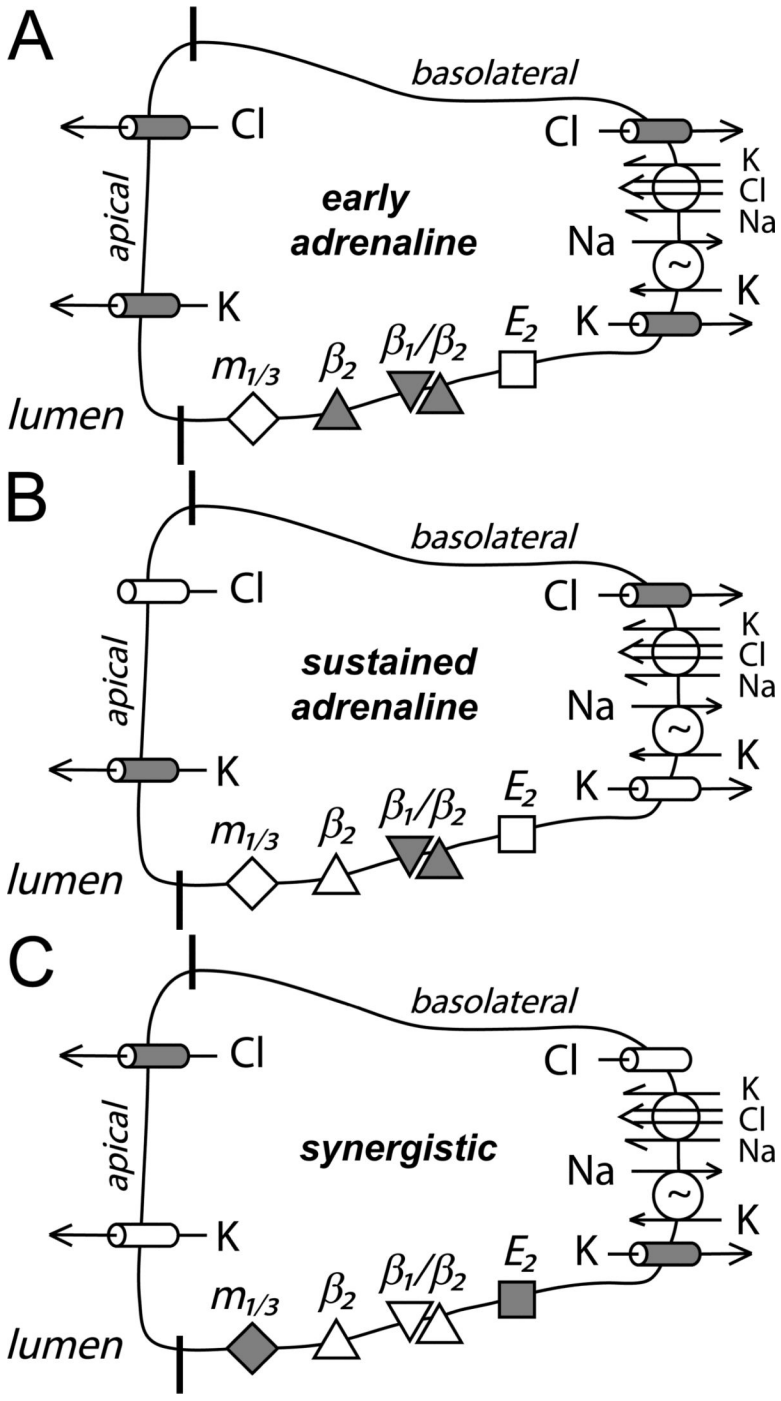

Figure 6. Cellular model for K^+ and Cl^- secretion

Schematic columnar cells of colonic epithelium show the transport steps required for electrogenic K^+-secretion and Cl^--secretion, with shading to emphasize the receptors and ion channels activated during each secretory mode. **A.** Early adrenaline activation (β2-AdrR and a β1-AdrR/β2-AdrR complex) includes opening of apical and basolateral membrane Cl^- and K^+ channels (*flushing mode*). A range of Cl^- and K^+ secretory rates would be possible with this activation scheme depending on relative channel opening and the resulting electrochemical driving forces. The observed positive I_{sc} (Fig 1A, control) indicates that β-

AdrR signaling produces a Cl^- secretory rate transiently higher than K^+-secretion, presumably due to greater apical membrane Cl^- channel activation. Inhibition of basolateral membrane Cl^- channels would be anticipated to result in higher rates of Cl^- exit across the apical membrane and a larger positive I_{sc} (Fig 3A). PGE_2 (E2-PtgR) activation also opens this same group of channels, in a manner that Cl^--secretion generally exceeds K^+-secretion (Rechkemmer *etal*., 1996). Inhibition of basolateral membrane Cl^- channels during this PGE_2 stimulated flushing mode also increases Cl^- exit across the apical membrane resulting in a larger positive I_{sc} (Fig 3B). **B.** Apical membrane Cl^- channels close during sustained adrenaline activation (β1-AdrR/β2-AdrR complex) such that only K^+-secretion persists (*modulatory mode*). The K^+ secretory rate can be altered by adjusting the ratio of apical K^+ conductance to basolateral K^+ conductance. Inhibition of basolateral membrane Cl^- channels would stop conductive Cl^- exit and thereby limit the negative I_{sc} associated with K^+-secretion (Fig 1B). **C.** Stimulation via combined muscarinic-(m1/3-AChR)/prostanoid-(E2-PtgR) activation (*synergistic mode*) closes basolateral membrane Cl^- channels which contributes to maximal Cl^--secretion, as supported by the lack of action by CaCCinh-A01 during this secretory mode (Fig 3C). The synergistic K^+ secretory rate is small compared with Cl^--secretion as indicated by the large positive I_{sc}, and may be similar in size to the K^+-secretion activated by PGE_2 alone.

Table 1

Action of Cl^- channel inhibitors

		CaCCinh-A01 30μM (n = 4)	GlyH-101 10μM (n = 4)	NPPB 10μM (n = 3)
adrenaline:	1st peak	↑ +101.9±21.0 {0.017}	↑ +48.3±9.1 {0.013}	↔ −15.8±61.5 {0.82}
	2nd peak	↑ +147.6±18.4 {0.004}	↑ +169.3±28.6{0.010}	↔ +11.5±27.5 {0.72}
	plateau	↓ +118.3±7.5 {0.001}	↓ *	↓ *
PGE_2:	1st peak	↑ +200.2±38.5 {0.014}	↑ +118.0±34.1{0.041}	↔ +13.1±86.5 {0.89}
	2nd peak	↑ +205.5±42.9 {0.017}	↑ +290.7±16.3{0.001}	↑ +95.6±21.1 {0.045}
	plateau	↑ +203.6±18.1 {0.002}	↔ +71.8±25.4 {0.07}	↑ +58.7±3.2 {0.003}
CCh/PGE_2:	1st peak	↑ +191.3±40.8 {0.018}	↓ −194.2±14.9{0.001}	↔ +75.7±31.1 {0.14}
	2nd peak	↔ +1.0±69.0 {0.98}	↓ −345.9±47.1{0.005}	↓ −98.3±15.7 {0.025}
	plateau	↔ −29.5±54.9 {0.63}	↓ −221.2±9.8 {0.001}	↓ −150.4±28.3 {0.034}

Secretagog activated I_{SC} were compared in the presence and absence of inhibitors (ΔI_{SC} = inhibitor – control; |μA/cm^2) for adrenaline (Fig 1A), PGE_2 (Fig 3B), and CCh/PGE_2 (Fig 3C). Significant increases in activation (stimulation, ↑) and decreases in activation (inhibition, ↓) are indicated {P values}.

* Data in Fig 1C.